Nanoscale

Effective delivery of a rationally designed intracellular peptide drug with gold nanoparticle-peptide hybrid

Journal:	*Nanoscale*
Manuscript ID:	NR-COM-04-2015-002377.R1
Article Type:	Communication
Date Submitted by the Author:	29-May-2015

Complete List of Authors:	Lee, Daiyoon; University Health Network, Zhao, Jinbo; The Fourth Military Medical University, Thoracic Surgery Yang, Hong; University Health Network, Thoracic Surgery Xu, Shuyun; University Health Network, Thoracic Surgery Kim, Hyunhee; University of Toronto, Physiology Pacheco, Shaun; University of Toronto, Physiology Keshavjee, Shaf; University Health Network, Thoracic Surgery Liu, Mingyao; University Health Network, Thoracic Surgery; University of Toronto, Physiology

Nanoscale

COMMUNICATION

Effective Delivery of a Rationally Designed Intracellular Peptide Drug with Gold Nanoparticle-Peptide Hybrids

Received 00th January 20xx,
Accepted 00th January 20xx

DOI: 10.1039/x0xx00000x

www.rsc.org/

Daiyoon Lee[a,b‡], Jinbo Zhao[a‡], Hong Yang[a], Shuyun Xu[a], Hyunhee Kim[a,c], Shaun Pacheco[a,c], Shaf Keshavjee[a,b], and Mingyao Liu[a,b,c]

A novel gold nanoparticle-peptide hybrid strategy was developed to intracellularly deliver a potent PKCδ inhibitor peptide for the treatment of acute lung injury. The gold nanoparticle-peptide hybrids showed good stability with high uptake, and demonstrated in vitro and in vivo efficacy. Our formulation strategy shows great promise in intracellular delivery of peptides.

Rational drug design has emerged as a new strategy to develop peptide-based drugs that can specifically regulate intracellular protein-protein interactions.[1] These rationally designed peptides act as mimetics to selectively facilitate or block the association between proteins. Intracellular delivery of these peptide-based drugs has been traditionally achieved through the conjugation of the therapeutic peptide to a cell-penetrating peptide (CPP), predominantly Tat peptide.[2] However, non-specific effects of Tat peptide have been reported, which present a significant concern in clinical practice.[3] Gold nanoparticles (GNPs) are particularly well-suited candidates for intracellular drug delivery because they possess a large surface area-to-volume ratio, good biocompatibility, low cytotoxicity, and their surface plasmon resonance optical property may be useful for GNP imaging in vitro and *in vivo*.[4, 5] GNPs have a high binding affinity to thiolated molecules, which provides an easy and effective way to modify GNP surface properties.[6] GNPs have been used to deliver a wide range of molecules, including siRNAs,[7] DNAs,[8] and proteins.[9] GNPs as a delivery tool for peptide-based drugs, however, have only been reported on peptides that target cell surface receptors.[10, 11]

To use GNPs as an intracellular peptide delivery vehicle, we have developed a novel peptide-GNP hybrid, composed of 20 nm spherical GNP coated with 95% P2 (CAAAAE) and 5% P4 (CAAAAW) peptides by molar ratio.[12] Compared to unmodified GNP, the 95P2P4-GNP-peptide hybrid demonstrated excellent stability in physiological saline solution and high cellular uptake.[12] In the present study, we used the 95P2P4-GNP hybrid as a delivery platform for a rationally-designed intracellular peptide drug, δV1-1, a non-toxic, highly isozyme specific PKCδ inhibitor.

PKCδ is a critical regulator of cell proliferation, immune response and pro-apoptotic signaling in many cell types.[13, 14] In the presence of apoptotic stimuli, such as genotoxins, death receptor activation or oxidative stress, PKCδ is activated through site-specific phosphorylation of its tyrosine residues. Activated PKCδ then translocates to subcellular organelles, including the nucleus, mitochondria, endoplasmic reticulum and lysosomes, by interacting with PKCδ-specific anchoring proteins called receptor-activated C kinases (RACKs). δV1-1 interferes with RACK-PKCδ interaction, thereby preventing PKCδ translocation to the subcellular compartments.[1, 15] In the absence of δV1-1, translocated PKCδ initiates apoptotic signaling by triggering caspase-3 activity in the mitochondria.[16, 17] Both activated and inactivated PKCδ can translocate to the nucleus and cause a number of changes including caspase-3-mediated DNA fragmentation and degradation of nuclear proteins, eventually leading to cell death.[18, 19] δV1-1 in the Tat peptide-conjugated form (named KAI-9803 and later Delcasertib) reduced ischemia-reperfusion induced organ injury in the heart and brain, and underwent phase II clinical trials for the treatment of cardiovascular diseases.[20] Considering the clinical trial was unsuccessful[21] and Tat's application as a delivery motif is limited due to non-specific effects,[3, 22] we examined whether δV1-1 can be effectively delivered using the 95P2P4-GNP hybridization strategy.

GNP-peptide hybrids were fabricated by incubating a pre-mixed 50 μM peptide stock solution in 50% acetonitrile with an aqueous solution of 20 nm spherical GNPs (Figure 1a). A cysteine residue was added at the N-terminus of the δV1-1 peptide (CSFNSYELGSL) as a gold binding motif. To optimize the therapeutic-to-stabilizing peptide ratio, GNPs with different peptide combinations were prepared and named from GNP-0PKCi to GNP-100PKCi (Figure 1c). The number in front of 'PKCi' indicates the percentage of δV1-1 in the peptide mixture, with the remaining peptides consisting of P2 and P4 at 95:5 molar ratio. We first tested the stability of GNP-peptide hybrids in physiologic ionic solution, since drugs administered intravenously are solubilized in 0.9% saline. The

‡ *Equal contribution*
[a] *Toronto General Research Institute, University Health Network, Toronto, ON, M5G 1L7, Canada.*
[b] *Institute of Medical Science, University of Toronto, Toronto, ON, Canada.*
[c] *Department of Physiology, University of Toronto, Toronto, ON, Canada.*
E-mail: mingyao.liu@utoronto.ca
Electronic Supplementary Information (ESI) available: Supplementary material includes the materials and methods section, and additional experiments to support the results in the main text. See DOI: 10.1039/x0xx00000x

stability of GNP-peptide hybrids decreased when the overall peptide concentrations were below 5 nM (Figure 1d), suggesting that this concentration is essential for peptides to stabilize GNP in the normal saline. When the percentage of 95P2P4 peptides was below 20%, namely in the preparations of GNP-80PKCi and GNP-100PKCi, the GNP-peptide hybrids became less stable in saline compared to that in the water, which also became apparent as the solution colour changed (Figure 1b, e and Supplementary Figure 1), suggesting that the P2/P4 peptides play important role for GNP-peptide hybrid stability in the saline. To estimate 20 nm GNP loading capacity, we developed a method using UV-Vis spectroscopy by taking advantage of the fact that Tyrosine or Tryptophan residues absorb light at 280 nm. Using GNP-100PKCi as an example, we found that 3,408 peptides attach per GNP, which was calculated to be 2.712 peptides/nm^2 GNP surface area (Supplementary Figure 2a). This is consistent with the value of 1.93 peptides/nm^2 for CALNN peptide, which was determined using amino acid analysis.[23] The stability of GNP-peptide hybrids is likely due to particle repulsion as all these preparations had a negative zeta potential between -25 and -30 mV (Supplementary Figure 2b).

We then studied whether the peptide coating is able to reduce serum protein adsorption on GNP, because adsorbed proteins may alter GNP surface chemistry and drug pharmacokinetics *in vivo*. Albumin, the most abundant serum protein, at 10 µM concentration increased the hydrodynamic size of unmodified GNP from 27 nm to 264 nm, while it had little effect on GNP-peptide hybrids (Figure 1f and Supplementary Figure 2c). Unmodified GNP showed a further size increase to 403 nm when incubated in fetal bovine serum (FBS) (Figure 1f) and a larger pellet was observed after centrifugation, an indication of high protein adsorption and GNP aggregation (Supplementary Figure 2c). FBS further increased the size of GNP-peptide hybrids (Figure 1f), which suggests that other proteins in the serum are able to interact with GNP and GNP-peptide hybrids. However, the sizes of GNP-peptide hybrids in the presence of FBS were below 83.2 nm.

Next, we used confocal microscopy to examine the cellular uptake of the GNP-peptide hybrids.[24] When aggregated 20 nm GNPs were excited with 633 nm laser, florescent emission was detected at 642-655 nm (Supplementary Figure 3a). Using the average intensity of confocal imaging collected from different cellular sections as an indirect measure (Supplementary Figure 3b), a high intensity signal was detected when human normal lung epithelial (BEAS2B) cells were incubated with GNP-0PKCi. The optical signal intensity decreased gradually with the increase in percentage of PKCi in the preparation (Figure 2 and Supplementary Figure 3c). We have previously demonstrated an association between this optical signal and GNP cellular uptake measured by ICP-MS.[12] Thus, the intensity differences indicate 95P2P4 peptides are required to facilitate the cellular uptake of GNP-peptide hybrids. Moreover, in our previous study, GNP-0PKCi was shown taken up by the cells through macropinocytosis as well as caveolae-mediated endocytosis.[12] Other GNP-peptide hybrids tested may utilize similar cellular internalization mechanisms. Once the GNP-peptide hybrids are inside the endocytic vesicles, it is speculated that cellular enzymes or the vesicular environment (such as the low pH) may release peptides from the gold nanoparticle, which may then escape into the cytoplasm. However, these steps need to be further studied.

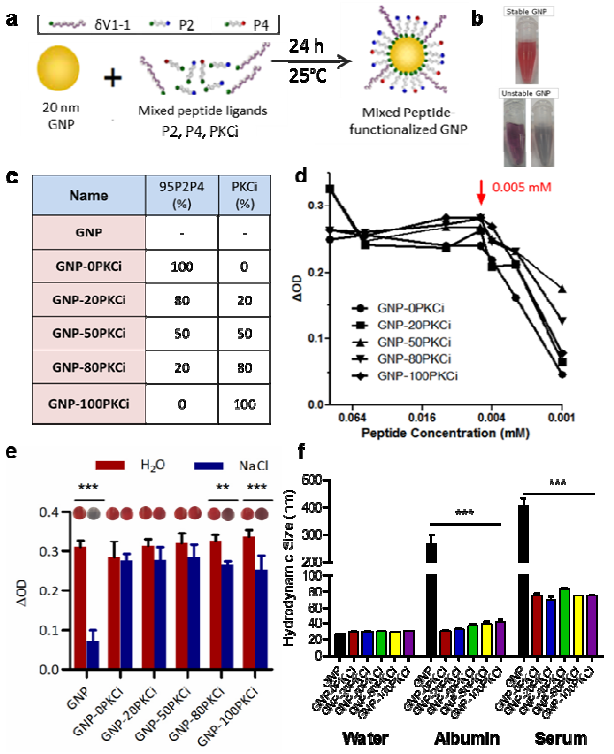

Figure 1. GNP-peptide hybrid design, fabrication and physicochemical characterization. (a) GNP-peptide hybrid fabrication using 20 nm GNP and rationally designed peptide ligands. (b) GNP-peptide hybrid preparations. (c) Examples of stable and unstable GNP-peptide hybrids. (d) The GNP-peptide preparations became unstable when the peptide concentrations were below 0.005 mM. PKCi and P2/P4 peptides were mixed at different ratios. Different concentrations of peptide mixtures were incubated with 1 nM GNP in 150 mM normal saline, and the stability of GNP-peptide hybrids was determined with UV-Vis spectrometry at 280 nm. ΔOD, representing the differences between the absorption at the peak and at the 440 nm (ΔOD = Apeak - A440), was determined by UV-Vis spectrophotometry. (e) When the PKCi concentrations were above 20% in the 50 µM peptide mixture, the stability of GNPs in 150 mM NaCl solution decreased. (See details in Supplementary Fig. 1). A decrease in ΔOD was accompanied by a solution colour change as seen in the top row of dots (**P < 0.01, ***P < 0.001, n = 4). (f) Protein adsorption on different nanoformulations, as determined by dynamic light scattering assay (***P < 0.001 vs. GNP alone, n = 3). The GNP-peptide hybrids also had a higher serum protein adsorption in FBS compared to water, but the increase in size was significantly less than GNP alone.

We then tested the therapeutic efficacy *in vitro* to screen out the most effective nanoformulation and to determine the most appropriate dose. A cell culture model that simulates the major features of ischemia-reperfusion process in lung transplantation was used.[25] Confluent human lung epithelial cells were subjected to cold ischemic time (CIT) in the presence of Perfadex®, a lung preservation solution, in an oxygen chamber to simulate physical conditions of lung preservation, followed by warm culture medium containing serum to simulate reperfusion (Figure 3a).[26] In the absence of CIT, none of the GNP-peptide hybrids showed any

noticeable cytotoxicity after treatment for 24 hours; there were no changes in cell density or morphology (Supplementary Figure 4). Subjecting lung epithelial cells to 18 hours of CIT followed by reperfusion resulted in a significant change in cell morphology (Figure 3b), and loss of cell viability (Figure 3c). GNP-20PKCi, GNP-50PKCi, and GNP-80PKCi, however, significantly rescued cells from apoptosis, while GNP-100PKCi (without delivery peptides), GNP-0PKCi (no therapeutic peptide), and δV1-1 peptide alone (without GNP) were not effective (Figure 3c). This demonstrates that a balance between 95P2P4 and PKCi peptide is critical in achieving optimal cellular uptake and consequently, therapeutic efficacy. GNP-50PKCi was chosen for further experiments because of its higher δV1-1 loading capacity than GNP-20PKCi. GNP-50PKCi improved cell viability in a dose dependent fashion (Supplementary Figure 5). GNP-50PKCi, but not GNP-0PKCi, affected PKCδ phosphorylation and expression levels of the total PKCδ (Figure 3d). Tat-PKCi and Tat alone were used as positive and negative controls for comparison (Figure 3c-d).

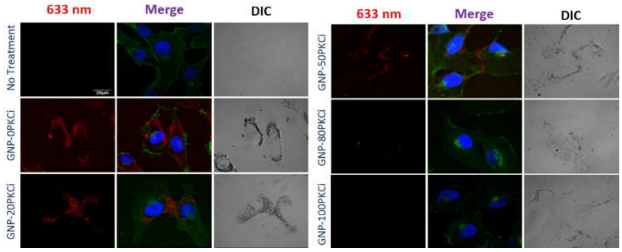

Figure 2. Cellular uptake of GNP-peptide hybrids estimated with confocal microscopy. BEAS2B cells were incubated with unmodified GNP or one of the hybrids for 2 hours and stained with Hoescht 33342 (blue) for the nucleus, and with WGA-Alex fluor 488 (green) to highlight the cytoplasm membrane. DIC image also shows intracellular GNP aggregates as black dots.

Under 6 hours of CIT, which simulates typical donor lung preservation period clinically, no major cellular morphology change and cell death were observed (data not shown). However, a strong inflammatory response was induced, with an increase in the production of pro-inflammatory cytokines and chemokines (Figure 3e-g). GNP-50PKCi significantly inhibited production of IL-6, IL-8 and GROα in a dose-dependent manner, which is consistent with studies that have previously reported the involvement of PKCδ in regulating airway inflammation.[27-29] Tat-PKCi was equally effective in inhibiting the production of pro-inflammatory cytokines. However, Tat alone also partially but significantly inhibited the production of IL-6 and GROα (Figure 3e, g), which provides further evidence of the non-specific effects of this delivery vehicle.

Before testing therapeutic efficacy of the nano-formulation *in vivo*, we evaluated the safety of GNP-50PKCi formula. Neither GNP-50PKCi nor GNP-0PKCi caused red blood cell aggregation (Supplementary Figure 6a). GNP-50PKCi (from 0.1 to 10 μM), GNP-0PKCi (10 μM) and Tat-PKCi (10 μM) did not induce hemolysis of red blood cells (Supplementary Figure 6b-c). GNP-50PKCi did not cause complement activation (Supplementary Figure 6d).

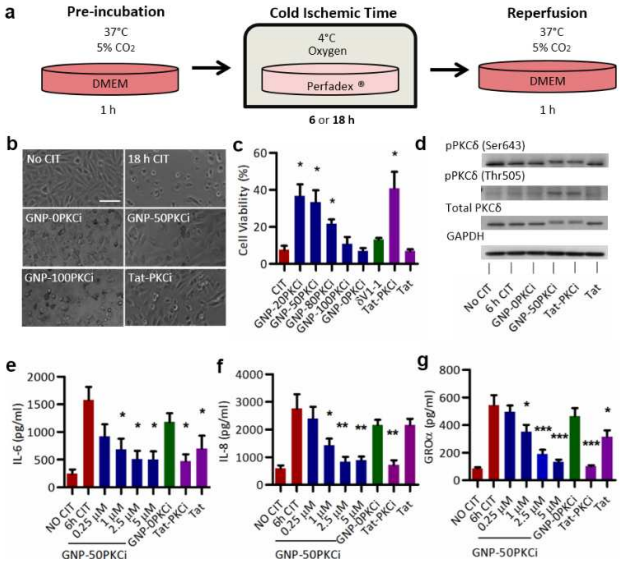

Figure 3. GNP-PKCi reduced ischemia-reperfusion (IR) induced inflammatory response and cell death in vitro. (a) A cell culture model to simulate IR-process of human lung preservation and transplantation. (b) GNP-50PKCi prevented IR-induced cell morphological change. GNP-100PKCi was less effective. GNP-0PKCi and Tat-PKCi were negative and positive control, respectively. Scale bar: 50 μm. (c) GNP-PKCi formulations significantly increased cell viability. The productive effect appears higher with more P2P4 delivery peptides in the formula (*P < 0.05 compared to CIT control, n = 3). (d) GNP-50PKCi affected PKCδ phosphorylation and stability. (e, f, g) GNP-50PKCi inhibited the production of cytokines (IL-6, IL-8 and GROα) in a dose-dependent manner (*P < 0.05, **P < 0.01, ***P < 0.001 compared to 6 h CIT control, n = 3). Non-specific inhibitory effects on IL-6 and GROα were noted in Tat-alone group.

To determine the protective effects of GNP-50PKCi *in vivo*, we used a rat pulmonary ischemia-reperfusion (IR) model with *in situ* left pulmonary ligation for 90 minutes, followed by 2 hours of reperfusion (Figure 4a). GNP-50PKCi (7.5 pmol/kg) was administrated intravenously 30 minutes before ischemia and immediately before reperfusion. GNP-50PKCi reduced congestion and hemorrhage in the left lung after ischemia-reperfusion (Figure 4b), improved lung oxygenation function with significantly higher PaO_2/FiO_2 ratio (Figure 4c), and reduced pulmonary edema shown as lower Wet/Dry lung weight ratio (Figure 4d).[30] GNP-50PKCi reduced the overall lung injury score, which was quantified based on alveolar wall thickening, intra-alveolar edema, neutrophil infiltration and intra-alveolar hemorrhage (Figure 4e, f). GNP-50PKCi-treated animals also had less TUNEL-positive apoptotic cells in the lung (Figure 4g, h). Although not statistically significant, there was a trend towards improved respiratory mechanics, measured as peak airway pressure, lung compliance, resistance and elastance, in the GNP-50PKCi treated animals (Supplementary Figure 7). All of these results indicate that GNP-50PKCi is a clinically applicable nanoparticle with potential to ameliorate ALI.

For comparison, Tat-PKCi at the dose previously used to treat cardiac infarction (0.1 mg/kg; equivalent to 20.4 pmol/kg)[31] offered limited therapeutic advantage after 90 minutes of ischemia and 2

hours of reperfusion (Supplementary Figure 8). Furthermore, Tat-alone treated animals developed severe lung injury and death (in 2 out of 5 rats) during reperfusion, which suggests that some of the off-target effects of Tat peptide could be detrimental. In a separate study, we found that Tat-δV1-1 demonstrated comparable protective effects after 60 minutes pulmonary ischemia (manuscript under revision), but its therapeutic effects were not as good as GNP-50PKCi when ischemia was increased to 90 minutes. Tat-δV1-1 has been shown to be effective in myocardial infarction[31, 32] and stroke [33, 34] in animal models, but its clinical trial results were not as good as expected.[21] We suspect this could be due to the short half-life of Tat-δV1-1[20] and off-target effects of Tat, both of which can be addressed with the GNP-peptide hybridization strategy.

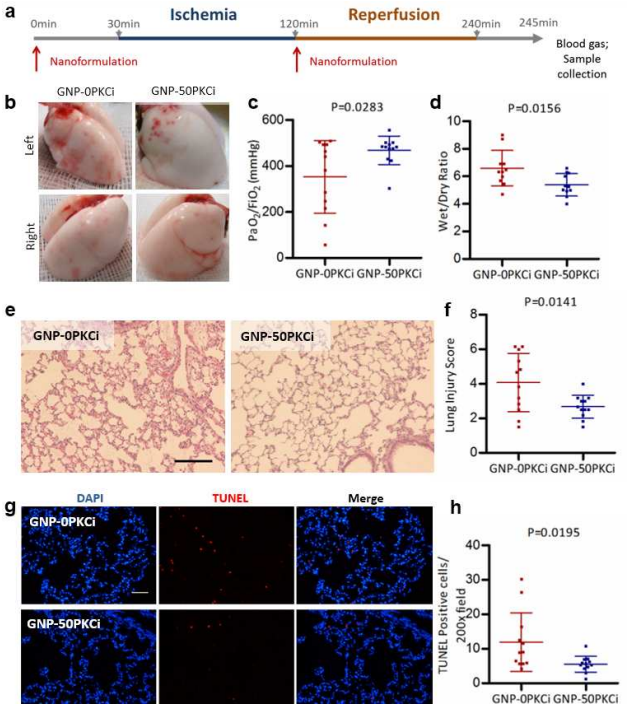

Figure 4. GNP-50PKCi reduced pulmonary ischemia reperfusion induced lung injury in rats. (a) Rat left lung ischemia-reperfusion model. (b) GNP-50PKCi reduced congestion of left lung after IR, in comparison with GNP-0PKCi-treated lungs. No difference was seen in the right lungs. (c) GNP-50PKCi improved oxygenation function of the left lung after reperfusion. (d) GNP-50PKCi reduced pulmonary edema, measured as wet-to-dry ratio of the left lung. (e) GNP-50PKCi reduced lung injury. Scale bar: 100 µm. (f) The lung injury score was significantly lower in the GNP-50PKCi treated group. (g) GNP-50PKCi reduced cell death. Scale bar: 100 µm. (h) GNP-50PKCi treated rats had a significantly lower TUNEL-positive apoptotic cells compared to GNO-0PKCi.

In comparison to chemical compounds, rationally designed peptide drugs, such as δV1-1, are much more target-specific. The development of GNP-peptide hybrids as an intracellular delivery tool provides an exciting new angle to peptide delivery, and this leaves an array of opportunities for further optimization. For example, specific targeting motifs may be added to this system for delivery into selective cell types. More importantly, our data suggests the same GNP-peptide hybridization technique can be applied to enhance the stability and therapeutic efficacy of many other peptide-based drugs to treat a wide range of diseases.

Notes and references

1. E. N. Churchill, N. Qvit and D. Mochly-Rosen, *Trends Endocrinol. Metab.*, 2009, 20, 25-33.
2. X. Zhang, X. Zhang and F. Wang, *Expert opinion on drug delivery*, 2012, 9, 457-472.
3. D. Lee, S. Pacheco and M. Liu, *Nanomedicine (Lond)*, 2014, 9, 5-7.
4. E. C. Dreaden, A. M. Alkilany, X. Huang, C. J. Murphy and M. A. El-Sayed, *Chemical Society reviews*, 2012, 41, 2740-2779.
5. E. Hutter and D. Maysinger, *Microsc. Res. Tech.*, 2011, 74, 592-604.
6. S. Rana, A. Bajaj, R. Mout and V. M. Rotello, *Adv Drug Deliv Rev*, 2012, 64, 200-216.
7. A. Elbakry, A. Zaky, R. Liebl, R. Rachel, A. Goepferich and M. Breunig, *Nano Lett.*, 2009, 9, 2059-2064.
8. J. S. Lee, P. A. Ulmann, M. S. Han and C. A. Mirkin, *Nano Lett.*, 2008, 8, 529-533.
9. D. R. Bhumkar, H. M. Joshi, M. Sastry and V. B. Pokharkar, *Pharm. Res.*, 2007, 24, 1415-1426.
10. L. Hosta-Rigau, I. Olmedo, J. Arbiol, L. J. Cruz, M. J. Kogan and F. Albericio, *Bioconjug. Chem.*, 2010, 21, 1070-1078.
11. A. Kumar, H. Ma, X. Zhang, K. Huang, S. Jin, J. Liu, T. Wei, W. Cao, G. Zou and X. J. Liang, *Biomaterials*, 2012, 33, 1180-1189.
12. H. Yang, S. Y. Fung and M. Liu, *Angew. Chem. Int. Ed. Engl.*, 2011, 50, 9643-9646.
13. M. Zhao, L. Xia and G. Q. Chen, *Arch. Immunol. Ther. Exp. (Warsz.)*, 2012, 60, 361-372.
14. A. Shukla, K. M. Lounsbury, T. F. Barrett, J. Gell, M. Rincon, K. J. Butnor, D. J. Taatjes, G. S. Davis, P. Vacek, K. I. Nakayama, K. Nakayama, C. Steele and B. T. Mossman, *Am. J. Pathol.*, 2007, 170, 140-151.
15. D. Mochly-Rosen, K. Das and K. V. Grimes, *Nat. Rev. Drug Discov.*, 2012, 11, 937-957.
16. M. G. Song, S. M. Gao, K. M. Du, M. Xu, Y. Yu, Y. H. Zhou, Q. Wang, Z. Chen, Y. S. Zhu and G. Q. Chen, *Blood*, 2005, 105, 3714-3721.
17. X. Qi, M. H. Disatnik, N. Shen, R. A. Sobel and D. Mochly-Rosen, *Mol. Biol. Cell*, 2011, 22, 256-265.
18. S. Kaul, A. Kanthasamy, M. Kitazawa, V. Anantharam and A. G. Kanthasamy, *Eur. J. Neurosci.*, 2003, 18, 1387-1401.
19. Y. Xie, *J. Mol. Cell. Biol.*, 2010, 2, 308-317.
20. Y. Miyaji, S. Walter, L. Chen, A. Kurihara, T. Ishizuka, M. Saito, K. Kawai and O. Okazaki, *Drug Metab. Dispos.*, 2011, 39, 1946-1953.
21. A. M. Lincoff, M. Roe, P. Aylward, J. Galla, A. Rynkiewicz, V. Guetta, M. Zelizko, N. Kleiman, H. White, E. McErlean, D. Erlinge, M. Laine, J. M. Dos Santos Ferreira, S. Goodman, S. Mehta, D. Atar, H. Suryapranata, S. E. Jensen, T. Forster, A. Fernandez-Ortiz, D. Schoors, P. Radke, G. Belli, D. Brennan, G. Bell, M. Krucoff and P. A. M. I. I. for the, *Eur. Heart J.*, 2014, DOI: 10.1093/eurheartj/ehu177.

22. H. Kim, S. Moodley and M. Liu, *Drug delivery and translational research*, 2015, 5, 275-278.
23. R. Levy, N. T. Thanh, R. C. Doty, I. Hussain, R. J. Nichols, D. J. Schiffrin, M. Brust and D. G. Fernig, *J. Am. Chem. Soc.*, 2004, 126, 10076-10084.
24. S. Klein, S. Petersen, U. Taylor, D. Rath and S. Barcikowski, *Journal of biomedical optics*, 2010, 15, 036015.
25. W. Gao, J. Zhao, H. Kim, S. Xu, M. Chen, X. Bai, H. Toba, H. R. Cho, H. Zhang, S. Keshavjeel and M. Liu, *J. Heart Lung Transplant.*, 2014, 33, 309-315.
26. J. A. Cardella, S. Keshavjee, E. Mourgeon, S. D. Cassivi, S. Fischer, N. Isowa, A. Slutsky and M. Liu, *J. Appl. Physiol.*, 2000, 89, 1553-1560.
27. K. Page, J. Li, L. Zhou, S. Iasvoyskaia, C. C. Corbit, J. W. Soh, B. Weinstein, A. R. Brasier, A. Lin and M. B. Hershenson, *J Immunol*, 2003, 170, 5681-5689.
28. R. Cummings, Y. Zhao, D. Jacoby, E. W. Spannhake, M. Ohba, J. G. Garcia, T. Watkins, D. He, B. Saatian and V. Natarajan, *J. Biol. Chem.*, 2004, 279, 41085-41094.
29. N. S. Holden, P. E. Squires, M. Kaur, R. Bland, C. E. Jones and R. Newton, *Cell. Signal.*, 2008, 20, 1338-1348.
30. J. E. Levitt, M. K. Gould, L. B. Ware and M. A. Matthay, *J. Intensive Care Med.*, 2009, 24, 151-167.
31. K. Inagaki, L. Chen, F. Ikeno, F. H. Lee, K. Imahashi, D. M. Bouley, M. Rezaee, P. G. Yock, E. Murphy and D. Mochly-Rosen, *Circulation*, 2003, 108, 2304-2307.
32. M. Tanaka, R. D. Terry, G. K. Mokhtari, K. Inagaki, T. Koyanagi, T. Kofidis, D. Mochly-Rosen and R. C. Robbins, *Circulation*, 2004, 110, II194-199.
33. W. H. Chou, D. S. Choi, H. Zhang, D. Mu, T. McMahon, V. N. Kharazia, C. A. Lowell, D. M. Ferriero and R. O. Messing, *J. Clin. Invest.*, 2004, 114, 49-56.
34. R. Bright, A. P. Raval, J. M. Dembner, M. A. Perez-Pinzon, G. K. Steinberg, M. A. Yenari and D. Mochly-Rosen, *J. Neurosci.*, 2004, 24, 6880-6888.

Table of Contents:

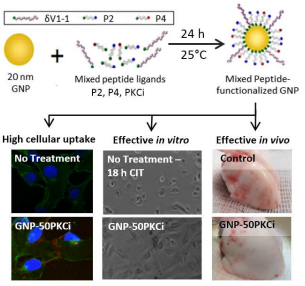

The paper reports a novel intracellular peptide delivery strategy using gold nanoparticle-peptide hybridization for the treatment of acute lung injury.